

MgB₂ Energy Gap Determination by Scanning Tunneling Spectroscopy

T.W. Heitmann^{1,2}, S.D. Bu³, D.M. Kim³, J.H. Choi³, J. Giencke³, C.B. Eom^{1,2,3}, K.A. Regan⁴,
N. Rogado⁴, M.A. Hayward⁴, T. He⁴, J.S. Slusky⁴, P. Khalifah⁴, M. Haas⁴, R.J. Cava⁴,
D.C Larbalestier^{2,3}, M.S. Rzchowski^{1,2}

¹*Physics Department, University of Wisconsin, Madison, WI*

²*Applied Superconductivity Center, University of Wisconsin, Madison, WI*

³*Dept. of Materials Science and Engineering, University of Wisconsin, Madison, WI*

⁴*Department of Chemistry and Princeton Materials Institute*

Princeton University, Princeton, NJ

We report scanning tunneling spectroscopy (STS) measurements of the gap properties of both ceramic MgB₂ and *c*-axis oriented epitaxial MgB₂ thin films. Both show a temperature dependent zero bias conductance peak and evidence for two superconducting gaps. We report tunneling spectroscopy of superconductor-insulator-superconductor (S-I-S) junctions formed in two ways in addition to normal metal-insulator-superconductor (N-I-S) junctions. We find a gap $\Delta=2.3$ - 2.8 meV, with spectral features and temperature dependence that are consistent between S-I-S junction types. In addition, we observe evidence of a second, larger gap, $\Delta=7.2$ meV, consistent with a proposed two-band model.

I. Introduction

Since its discovery as a superconductor with $T_c=39$ K by Akimitsu et al[1], magnesium diboride has garnished considerable interest. Unlike most known superconductors, MgB₂ is a metallic binary compound with a relatively simple layered hexagonal crystal structure. Its relatively high T_c coupled with its simple structure (hence, ease of processing) and high critical current density[2] make MgB₂ an attractive candidate for practical applications. This has rejuvenated interest in the search for other similar materials, possibly with further enhanced properties. Some materials with related structure and otherwise similar properties have already been reported to

superconduct[3,4,5], but all with lower transition temperatures.

Although MgB₂ may not fall neatly into either conventional or high temperature superconducting classes, it appears to be most similar to the conventional superconductors[6] but with a critical temperature far surpassing the 23 K T_c of Nb₃Ge. Experiments have shown MgB₂ to exhibit a boron isotope effect [7,8], suggesting that phonons play an important role in electron-electron coupling. Specific heat measurements support phonon mediated coupling[9], but positive hall coefficients have been measured, more typical of high- T_c superconductors[10]. In addition, the gap symmetry of MgB₂ remains controversial.

Scanning tunneling spectroscopy (STS) is an excellent probe of the density of states in a superconductor. In particular, the differential conductance obtained through STS can determine the superconducting gap (Δ) with a resolution much less than $k_B T$. Zero bias conductance peaks and other mid-gap states contain further information concerning the tunneling properties.

A number of tunneling spectroscopy measurements on MgB_2 have thus far been reported in the literature[11,12,13,14,15,16,17,18,19,20,21]. The results are varied and a consistent picture of the tunneling process on these materials has yet to be established. Reported values of the gap range from less than 2 meV to about 7.5 meV[11-19], well below and above the $\Delta=5.9$ meV value predicted from BCS weak coupling, $2\Delta/k_B T_C=3.52$. Most commonly reported gap values cluster around 2, 4, and 7 meV. In addition to variation in the magnitude, multiple gap features have been reported by some authors[12,18,19,20].

The existence of a double gap has been proposed to result from Cooper pairs associated with different sheets of the Fermi surface[22,23,24]. In this picture, two nearly-independent gap functions are weakly coupled such that they close at the same T_C . Of these two gaps, it is believed that one appears predominantly in the boron plane due to σ -bonded boron p_x and p_y orbitals, and the other results from the more three dimensional, π -bonded p_z orbitals. A directional dependence in the tunneling then arises from the dimensionality of the orbitals associated with the particles in each band. Tunneling into the p_z orbitals is nearly isotropic, whereas tunneling into the p_x and p_y orbitals is strongest for wavevectors in the boron plane. Thus, directional tunneling measurements may be necessary to elucidate the nature of such double gap features. A recent report[20] suggests that spectral

features are dependent on the directional configuration of the tunneling junction.

II. Experiment

We report STS measurements of the gap properties of ceramic MgB_2 and *c*-axis oriented epitaxial MgB_2 thin films in both S-I-S and normal metal-insulator-superconductor (N-I-S) configurations. Both show a temperature-dependent zero-bias conductance peak and evidence of two superconducting gaps. One of the S-I-S type junctions resulted from inadvertently touching the normal metal Pt-Ir tip to the surface of a bulk ceramic MgB_2 sample. This led to tunneling between a piece of MgB_2 on the tip and the MgB_2 sample itself. We refer to this junction type as “type A” S-I-S junction. Ceramic samples were produced by direct reaction of Mg flakes with amorphous B powder, pressed into pellets, and fired (1 hour each at 600, 800, and 900° C) on a Ta foil[2].

The second type of S-I-S junction was prepared by affixing a piece of the ceramic sample to the Pt-Ir wire with Ag epoxy, thus forming a superconducting tip. This tip was then used for tunneling spectroscopy of an epitaxial, *c*-axis oriented MgB_2 thin film. This junction type will be referred to as “type B” S-I-S junction. We also performed N-I-S spectroscopy on the film using a Pt-Ir tip to independently determine its gap value. The thin film was grown by RF magnetron sputter deposition of amorphous B on (0001) Al_2O_3 , followed by an anneal in Mg vapor at 850°C [25].

Tunneling characteristics were acquired using an Oxford Instruments CryoSTM in scanning tunneling microscopy (STM) mode from 5 K to 35 K. The sample and STM head are in the flowing He gas of a gas flow cryostat. The cryostat is mounted in an acoustically isolated enclosure supported by a vibration isolation table. Differential conductance (dI/dV) vs. bias voltage scans

were obtained using a standard lock in technique. Voltage was quickly swept with the z -position feedback off in order to maintain a fixed position for the duration of each dI/dV . STM tips were mechanically prepared from 250 μm diameter Pt-Ir alloy wire, and also by attaching a piece of ceramic MgB_2 to the Pt-Ir wire.

Spectra were obtained at temperatures from 5 K to 30 K from the as-grown pellet for type A S-I-S junctions, and up to 35 K for type B S-I-S junctions. The N-I-S spectra of the film were obtained at $T=5$ K. In all cases, either altered surface structure or an impurity surface layer may have influenced the tunneling properties.

In the type A S-I-S junctions we were not able to maintain tunneling during some temperature changes, and found that the tip would occasionally touch the surface, potentially picking up a piece of the superconducting sample. This possibility requires us to discern the N-I-S or S-I-S nature of the junction from the dI/dV measurement. We will show that these junctions are in fact S-I-S based on their temperature dependent zero bias conductance peaks and consistency with prepared type B S-I-S junctions spectra at all temperatures. Some searching on the sample surface was necessary to obtain good tunneling conditions, obtained through topographic imaging and $I(V)$ sampling. The surface of our sample was found to be rough and only in some regions was consistent tunneling possible. In these regions of the sample we were able to achieve low noise tunneling with very consistent gap values and spectral features in general. In some regions we found $\Delta(T)$ to be approximately independent of position within experimental error, and in other regions the $I(V)$ were consistently Ohmic.

As an aid in determining the junction type of the type A S-I-S junction we also performed S-I-S tunneling of type B S-I-S

junctions consisting of an MgB_2 grain fabricated onto a tip tunneling into an MgB_2 thin film. We observed spectra consistent with the type A S-I-S junction at all temperatures including temperature dependent zero bias conductance peaks and similar gap values and spectral shapes with additional features for some spectra indicative of a second, larger gap (see section V). We attribute the presence of these features in only some but not all spectra to directional dependence of tunneling. We also performed N-I-S tunneling measurements on the film to independently determine its superconducting gap.

III. Data

Our dI/dV curves for the type A S-I-S junctions exhibit a number of clear features and trends. We observe a nearly temperature-independent energy gap up to 30 K and a zero bias conductance peak (ZBCP) that increases with temperature. Most spectra have dips at voltages just greater than the gap energy as well as a sub-gap structure more 'V'-shaped than one would expect for a BCS superconductor.

Each spectrum represents an average of typically 20 bias-voltage scans. The z -position feedback is off for the entire duration of the series of averaged scans (about 10 seconds). Our STM is especially vibration sensitive due to its very long piezoelectric scan tube, capable of attaining 8 μm scans at 4 K. Averaging accentuates features common between scans and consequently attests to the consistency of measurement and to the validity of the features present in the spectra. At low temperatures our data exhibit very sharp gap features, clearly identifiable gap features for higher temperatures, and ZBCPs that become more prominent with increasing temperature. Figure 1 shows an STS spectrum at 5 K with fits using the N-I-S Blonder, Tinkham, Klapwijk (BTK) model ($\Delta=3.9$ meV) or S-I-S BCS model

($\Delta=1.9$ meV) (see Section V for details of the models). In both cases the gap is much smaller than the weak coupling limit.

Figure 2 shows an N-I-S spectrum of the MgB_2 film obtained with a Pt-Ir tip. This spectrum is fit with the N-I-S BCS model for the dI/dV as described in section V with $\Delta_s=2.3$ meV and phenomenological smearing parameter $\Gamma=0.8$. Note that the peaks occur at voltages slightly larger than Δ as obtained from the fit. This is due to broadening effects as is evidenced by the model. We find that matching peak heights of the fit curve to the data results in the most reliable gap values. Discrepancies between the fit and the data suggest the presence of mid-gap states not taken into account by the gap-smeared density of states. Gap values obtained from the peak position of sharply peaked gap features agree quite well with gap values obtained from fitting. Due to variable spectral shapes, including multiple gap features in some spectra, we were unable to fit all of the data. Therefore, average gap values we report here are obtained from peak locations. This leads to slightly inflated, but fairly representative values of the gap. These spectra are consistent with an N-I-S junction and in none of the spectra did we find evidence for picking up a piece of MgB_2 from the film surface.

The type B dI/dV curves displayed characteristics similar to those for type A, and also, in some configurations, peaks at voltages consistent with $\Delta_s+\Delta_L$ from the two-band model. Here, Δ_s is the small gap associated with the π -band and Δ_L is the large gap associated with the σ -band. These different configurations are experimentally found at different locations on the sample, or at different tunneling distances. We argue that they arise from tunneling from different locations on the surface of the fabricated MgB_2 tip. Transitions between tunneling locations on the tip are not unusual in scanning tunneling microscopy, and can be

attributed to imperfect topography of the tip. Figure 3 shows a dI/dV characteristic with very similar shape as for type A. A BCS S-I-S fit is also shown, and it gives a similar result for the gap, $\Delta_s=2.4$ meV. Figure 4 shows two dI/dV characteristics with features indicative of two gaps. Although the spectra display dramatically different shapes, the gap features appear at nearly the same bias voltages in the two curves. We argue that the second gap feature observed should be associated with $\Delta_s+\Delta_L$, and its presence indicates that the piece of MgB_2 on the tip is oriented such that tunneling takes place through its a - b plane, as per the discussion in Section I. No peaks associated with $2\Delta_L$ were ever observed, consistent with the c -axis orientation of the film. The average gap values obtained from spectra of this type are $\Delta_s=2.8$ meV and $\Delta_L=7.2$ meV.

IV. General Observations

We measure an approximately constant superconducting gap for all tip locations and temperatures up to 30 K for both the ceramic sample and the epitaxial thin film. Figure 5 shows the mean gap measured at each temperature, indicating that there is little temperature dependence within our statistical error. However, the ZBCP changes dramatically with temperature and varies only slightly between different tip locations on the sample at the same temperature. Figure 4 shows that the magnitude of the ZBCP generally increases with increasing temperature. ZBCPs can result from a number of mechanisms, but most mechanisms lead to a ZBCP that increases in magnitude as the temperature decreases[26]. Based on the temperature dependence of our data and consistency with the type B data we will argue that the ZBCPs arise from an S-I-S tunneling configuration.

Deviations from BCS behavior for the dI/dV include a more ‘V’-shaped sub-gap structure, finite zero bias conductance, a

ZBCP (consistent with S-I-S but not N-I-S), and a dip and hump feature for voltages just greater than the gap. The conductance drops to its lowest value within the gap less rapidly than predicted by the BCS density of states. This suggests the presence of mid-gap states associated with a surface impurity layer[27] on the MgB_2 . At all temperatures, some tunneling current is observed inside the gap. Although it may be reasonable at 5 K to attribute this to non-zero temperature, we find that this picture is inadequate at higher temperatures. In particular, Fig. 6 shows that the zero-bias conductance can be quite large at high temperatures. Zero-bias tunneling may result from Andreev reflections in the case of low impedance N-I-S tunneling as described by the BTK model[28], and ZBCPs may result from matching of peak density of states in the energy spectra between superconductors in the case of S-I-S tunneling, as discussed recently[21]. Note, also, the dip and hump feature for voltages of about 9 meV in Figs. 1 and 3. It has been suggested[21] that this feature is due to interband quasiparticle exchange in a two-band superconductor. This feature of the data may then be interpreted as evidence for a second gap.

V. Analysis

We have evaluated our type A S-I-S junction data using a BCS density of states, and three models for the tunneling characteristic, N-I-S, BTK, and S-I-S. BTK and S-I-S fits are shown in Fig. 1. For all fits we use a modified BCS DOS,

$$N(E) = \text{Re} \frac{|E - i\Gamma|}{\sqrt{(E - i\Gamma)^2 - \Delta^2}}, \text{ where } \Gamma \text{ is a}$$

smearing parameter. This is proportional to the N-I-S dI/dV at zero temperature. Both the N-I-S and S-I-S models were fit with the expression,

$$\frac{dI}{dV} = \int \frac{d}{dV} N(E) N(E + V) [f(E) - f(E + V)] dE$$

, where $N(E)$ is as given above and $f(E)$ is the Fermi function. For N-I-S tunneling, $N(E+V)$ is just the constant DOS for the normal metal at the Fermi level and is absorbed in the normalization. The S-I-S model is described by the entire expression with both DOS superconducting. This is formally where the two models differ. The fit expression for BTK is given by

$$\frac{dI}{dV} = G_0 \int \frac{d}{dV} [f(E + V) - f(E)] [1 + A(E) - B(E)] dE$$

, where G_0 is the normal state conductance. Here, the density of states is contained in the coefficients $A(E)$ and $B(E)$, which represent Andreev reflection and normal reflection, respectively. Details of the BTK model can be found in reference [28], from which we have used the general form for the transmission coefficients $A(E)$ and $B(E)$. We used a smearing parameter of $\Gamma=0$ in the DOS when fitting with the BTK model.

Type A Junctions: Ceramic MgB_2 -Insulator-Ceramic MgB_2

For our type A junction data we find that, even at low temperature, the N-I-S model (not shown in Fig. 1) does not fit well and for higher temperatures fails altogether. We concluded that our junction has a more complicated tunneling characteristic and applied the BTK N-I-S model for vacuum tunneling in its general form, appropriate for low impedance junctions. The tunneling impedance for our junctions are typically 150 $\text{M}\Omega$, comparable to that obtained elsewhere for MgB_2 N-I-S junctions[4]. Our 5 K data fits satisfactorily to this model with $\Delta=3.9$ meV (approximately twice the gap value of our later S-I-S interpretation) and dimensionless barrier strength $Z=5.0$, where we have used the ambient measurement temperature for T in the Fermi function (see Fig. 1). However, this model does not account for the ZBCP detected at all temperatures above 5 K (see Fig. 6). If the junction is N-I-S, then we conclude that BTK only describes

part of the characteristic and we must consider deviations from the ideal case described by the model. Narrowing of the gap at low voltages may result from mid-gap states[27]. This latter feature is consistent throughout our data but none of the N-I-S models considered can directly account for them. Mid-gap states are likely to exist because of surface layer effects, whether they are strain induced lattice defects at the surface or a layer of reacted or adsorbed impurity material.

An N-I-S junction with mid-gap states and bound state Andreev reflection would produce a ZBCP[17,27]. However, this is not consistent with our measured temperature dependence. In the absence of Andreev bound-state effects, mid-gap states can in some cases produce zero bias anomalies but those features would also persist above T_c [27]. This is not the case in our measurements.

In light of the possibility of having a piece of MgB_2 on the STM tip we also fit our data with the BCS model for an S-I-S junction. Our 5 K data were fit using $T=5$ K in the Fermi function and smearing parameter $\Gamma=0.35$ meV, determined by manually optimizing the numerical integration of the model dI/dV . This picture is more consistent with our data and qualitatively accounts for the temperature dependence of the ZBCP. This can be seen by considering the semiconductor model of S-I-S tunneling. In this model, peaks in the dI/dV will occur at $\pm(\Delta_1+\Delta_2)$ and $\pm(\Delta_1-\Delta_2)$, with Δ_1 and Δ_2 the gap values of the potentially dissimilar superconducting electrodes. In the case of two superconductors of the same material, $\Delta_1=\Delta_2\equiv\Delta$, $eV=\pm(\Delta_1-\Delta_2)=0$ corresponds to the ZBCP. The temperature dependence of the ZBCP results from thermally excited quasiparticles in one superconducting electrode tunneling into empty states above the gap of the other superconductor. At zero temperature, the complete absence of

quasiparticles suppresses the ZBCP. Higher temperatures provide the thermal energy necessary to excite more quasiparticles, increasing the ZBCP. The peak in the dI/dV occurs at zero bias due to the peaked nature of the DOS at the gap edge. Peaks at $\pm(\Delta_1+\Delta_2)=2\Delta$ results from Cooper pair breaking with one quasiparticle tunneling immediately while the other is promoted to lower lying quasiparticle states in the same superconductor. Since this supplies more carriers for tunneling, the peak at 2Δ is larger than the ZBCP.

Type B Junctions: Ceramic MgB_2 -Insulator-Epitaxial MgB_2 Thin Film

Figure 7 shows the mean gap measured at each temperature up to 35 K for type B junctions. Again, the gap is approximately constant up to 30 K, consistent with our observations for type A junctions. The value of the gap is also consistent with the S-I-S interpretation of the hottype A junctions. Figure 8 displays offset dI/dV curves for this junction type at all measured temperatures. The spectral shape, including ZBCPs and the dip and hump feature, as well as peak heights and locations closely resembles those for type A. We take this consistency as strong evidence for the S-I-S tunneling interpretation of the type A junctions on bulk ceramic material.

The semiconductor model of S-I-S tunneling suggests that peaks should occur at the sums and differences of the gaps. Multiple gap features in some of our data are consistent with this two gap picture. In the context of a double gap superconductor we would expect peaks in the dI/dV for voltages of $\pm 2\Delta_s$, $\pm(\Delta_s+\Delta_L)$, $\pm 2\Delta_L$, and $\pm(\Delta_s-\Delta_L)=\pm(\Delta_L-\Delta_s)=0$. We, however, have not observed $\pm 2\Delta_L$ and only in some spectra do we observe $\pm(\Delta_s+\Delta_L)$. It has been suggested that, due to tunneling matrix elements, the small gap is more geometrically favorable to appear from a random junction orientation than is the large

gap[20]. Spectra exhibiting only the peaks at $\pm 2\Delta_s$ are consistent with predominantly c-axis tunneling and those spectra also exhibiting peaks at $\pm(\Delta_s + \Delta_L)$ are consistent with an $a-b$ plane component from the tunneling tip. From the geometric, matrix element considerations presented in section I it is then clear that we should, in fact, *not* observe $\pm 2\Delta_L$ due to the c-axis orientation of the film. As we have discussed above, the ZBCP is temperature dependent and thus its presence or absence in any spectrum is determined by temperature. That leaves $\pm(\Delta_s - \Delta_L)$, which happens to be approximately equal to $\pm 2\Delta_s$. We argue that the $\pm(\Delta_s - \Delta_L)$ peak is obscured by the stronger $\pm 2\Delta_s$ peak, though some broadening will result, since Δ_s^{bulk} is not exactly equal to Δ_s^{film} . The T_c of the film (35 K) is slightly depressed from the bulk value (39 K), which means that the gap of the film should also be slightly depressed from the bulk value. By comparing Figs. 1 and 3 we notice that some additional broadening occurs when tunneling takes place between bulk and film.

VI. Conclusions

In summary, we have measured the superconducting gap of bulk and thin film MgB₂ by low temperature scanning tunneling spectroscopy in both S-I-S and N-I-S configurations. The gap determined from an overall average of our 5 K measurements is $\Delta=2.3$ meV, smaller than the BCS weak coupling limit, and varies little with temperature up to $T/T_c=0.77$. We have also observed evidence for a second, larger gap ($\Delta_L=7.2$ meV) for prepared S-I-S junctions. The simple semiconductor picture extended to the two-band superconductor model successfully describes the peak locations in our data. The detailed shape of the spectra, including the dip and hump feature observed just above the gap features, are not well-modeled by any of the fits investigated here, and may arise through microscopic

mechanisms not considered here. The most ubiquitous ‘non-gap’ feature we have observed, the dip and hump structure, has recently been attributed to a form of interband interaction[21]. We do not have an understanding of the other more subtle shape differences between spectra. However we do observe that gap features are robustly independent of the detailed spectral shape, and give a consistent representation of the gap structure in MgB₂.

Work at the University of Wisconsin was supported by the NSF MRSEC on Nanostructured Materials.

References:

- 1 J. Nagamatsu, N. Nakagawa, T. Muranaka, Y. Zenitani, and J. Akimitsu, *Nature* **410**, 63, (2001)
- 2 D.C. Larbalestier, et al, *Nature* **410**, 186 (2001).
- 3 D. Kaczorowski, A.J. Zaleski, O.J. Zogal, and J. Klamut, *cond-mat/0103571*
- 4 V.A. Gasparov, N.S. Sidorov, I.I. Zver’kova, and M.P. Kulakov, *JETP Lett.* **73**, 532 (2001).
- 5 D.P. Young, R.G. Goodrich, P.W. Adams, J.Y. Chan, and F.R. Fronczek, F. Drymiotis, L.L. Henry, *Phys. Rev. B* **65**, 180518 (2002).
- 6 C. Buzea and T. Yamashita, *Supercond Sci. Tech.* **14**, R115 (2001).
- 7 S.L. Bud’ko, G. Lapertot, C. Petrovic, C.E. Cunningham, N. Anderson, and P.C. Canfield, *Phys. Rev. Lett.* **86**, 1877 (2001)
- 8 D.G. Hinks, H. Claus, and J.D. Jorgensen, *Nature* **411**, 457 (2001)
- 9 R.K. Kremer, B.J. Gibson, and K. Ahn, *Cond-mat/0102432v2*
- 10 R. Jin, M. Paranthaman, H.Y. Zhai, H.M. Christen, D.K. Christen, and D. Mandrus, *Phys. Rev. B* **64**, 220506 (2001)
- 11 G. Rubio-Bollinger, H. Suderow, and S. Vieira, *Phys. Rev. Lett.* **86**, 5582 (2001)

12 F. Giubileo, D. Roditchev, W. Sacks, R. Lamy, and J. Klein, *Europhys. Lett.* **58**, 764 (2002)

13 G. Karapetrov, M. Iavarone, W.K. Kwok, G.W. Crabtree, and D.G. Hinks, *Phys. Rev. Lett.* **86**, 4374 (2001)

14 P. Seneor, C.T. Chen, N.C. Yeh, R.P. Vasquez, L.D. Bell, C.U. Jung, M.S. Park, H.J. Kim, W.N. Kang, S.I. Lee, *Phys. Rev. B* **65**, 12505 (2002).

15 A. Plecenik, S. Benacka, and P. Kus, *Physica C* **368**, 251 (2002)

16 Y. Zhang, D. Kinion, J. Chen, and John Clarke, D.G. Hinks and G.W. Crabtree, *Appl. Phys. Lett.* **79**, 3995 (2001).

17 H. Schmidt, J.F. Zasadzinski, K.E. Gray, and D.G. Hinks, *Phys. Rev. B* **63**, 220504 (2001)

18 F. Laube, G. Goll, J. Hagel, H.v. Lohneysen, D. Ernst, and T. Wolf, *Europhys. Lett.* **56**, 296 (2001).

19 P. Szabo, P. Samuely, J. Kacmarcik, Th. Klein, J. Marcus, D. Frunchart, S. Miraglia, C. Marcenat, and A.G.M. Jansen, preprint

20 M. Iavarone, G. Karapetrov, A.E. Koshlev, W.K. Kwok, G.W. Crabtree, and D.G. Hinks, *cond-mat/0203329*

21 H. Schmidt, J.F. Zasadzinski, K.E. Gray, and D.G. Hinks, *Phys. Rev. Lett.* **88**, 127002 (2002)

22 A.Y. Liu, I.I. Mazin, J. Kortus, *Phys. Rev. Lett.* **87**, 87005 (2001); H.J. Choi, D. Roundy, H. Sun, M.L. Cohen, G. Louie, *cond-mat/0111183*.

23 I. Hase and K. Yamaji, *J. Phys. Condensed Matter* **14**, 371 (2002)

24 K. Yamaji, *J. Phys. Soc. Jpn.* **70**, 1476 (2001)

25 S.D. Bu, et al, *Appl. Phys. Lett.*, accepted.

26 E.L. Wolf, *Principles of electron tunneling spectroscopy*, Oxford University Press, (New York, 1985).

27 J. Halbritter, *Appl. Phys. A* **68**, 153 (1999)

28 G.E. Blonder, M. Tinkham, and T.M. Klapwijk, *Phys. Rev. B* **25**, 4515, (1982)

Figure 1. Differential conductance of ceramic MgB_2 at 5 K for the type A S-I-S junction (data are closed circles) with fits to BTK (dashed line; $\Delta=3.9$ meV, $Z=5.0$) and BCS S-I-S junction (solid line; $\Delta=1.9$ meV, $\Gamma=0.35$ meV) models. Note that although the peaks match reasonably well, both models are slightly more ‘U’-shaped than is our data. Also, for the S-I-S junction a ZBCP begins to emerge already at 5 K. This feature of the S-I-S picture is more consistent with our higher temperature data.

Figure 2. Differential conductance of MgB_2 thin film (data are closed circles) with BCS N-I-S fit with $\Delta=2.3$ meV and smearing $\Gamma=0.8$. (fit is solid line).

Figure 3. Differential conductance of ceramic MgB_2 at 5 K for the type B S-I-S junction (data are closed circles) with a BCS S-I-S fit with $\Delta=2.4$ meV and $\Gamma=0.6$. Note the striking similarity with Figure 1.

Figure 4. Two overlaid differential conductance curves of ceramic MgB_2 at 5 K for the type B S-I-S junction. These data display the consistency with which multiple gap features appear at the same voltages despite different peak heights. The dashed lines are guides to the eye.

Figure 5. Temperature dependence of the superconducting gap for the type A S-I-S junction averaged for all data at each temperature. Error bars are one sigma.

Figure 6. Representative dI/dV curves of the type B S-I-S junction for the as grown sample for temperatures ranging from 5 K to 25 K (offset for clarity (2 units for 10 K curve and 1 unit for each additional temperature change)). Note the general trend of increasing ZBCP height with increasing temperature and the relatively constant gap width.

Figure 7. Temperature dependence of the superconducting gap for the type B S-I-S junction averaged for all data at each temperature. Error bars are one sigma.

Figure 8. Representative dI/dV curves of the type B S-I-S junction for the MgB_2 thin film for temperatures ranging from 5 K to 35 K (offset for clarity (2 units for 10 K curve and 1 unit for each additional temperature change)). Note the striking similarity to Fig. 6 in the general trend of increasing ZBCP height with increasing temperature and the relatively constant gap width.

Figure 1
Heitmann, et al

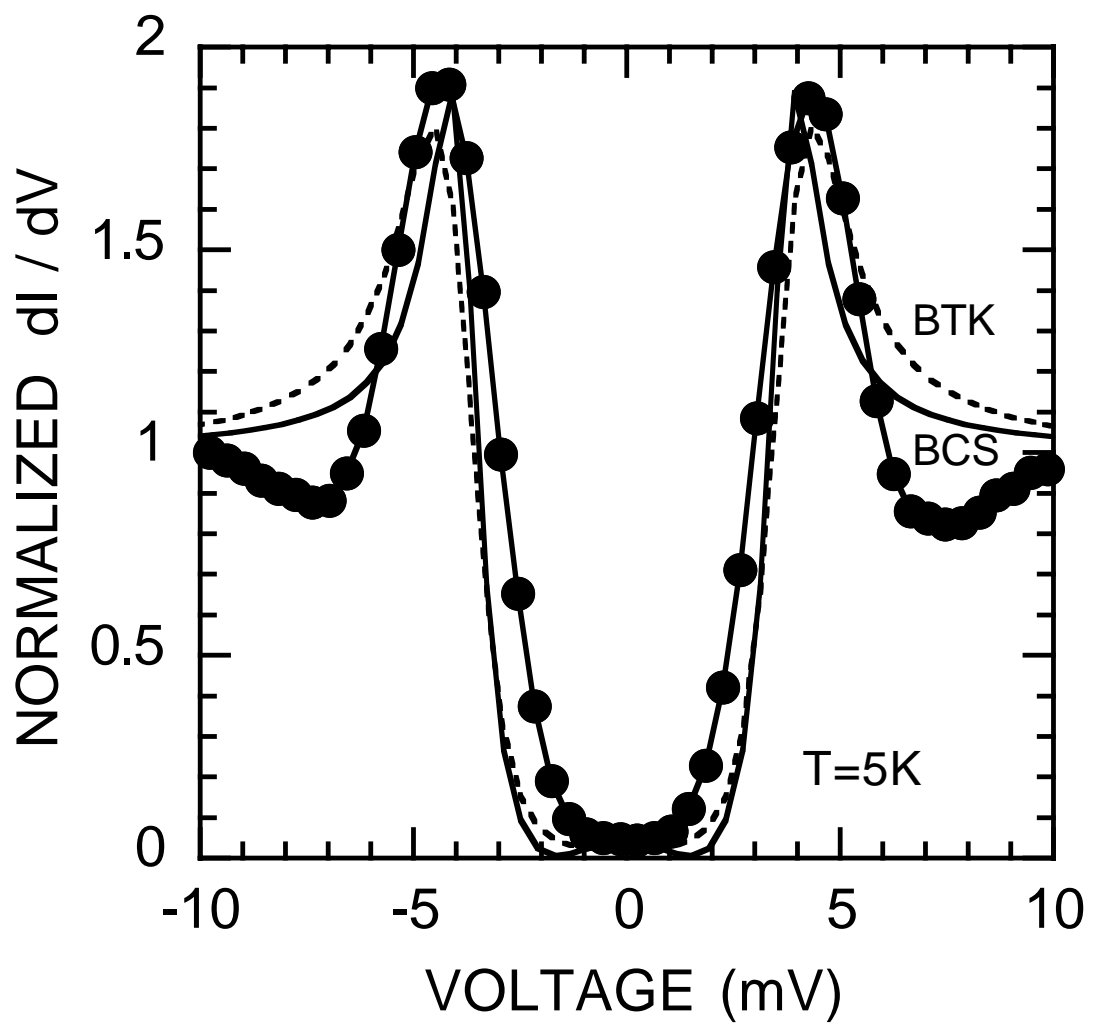


Figure 2
Heitmann et al

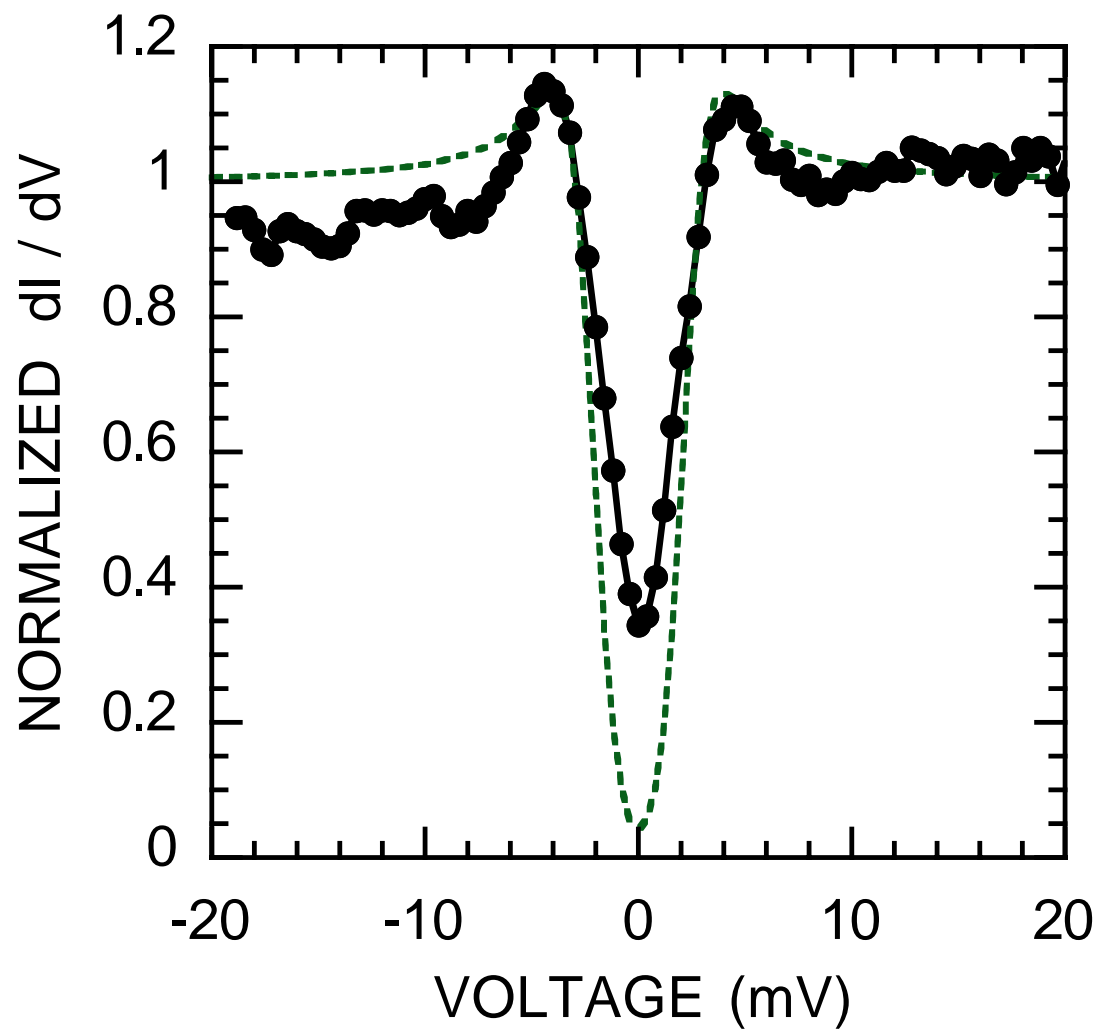


Figure 3
Heitmann et al

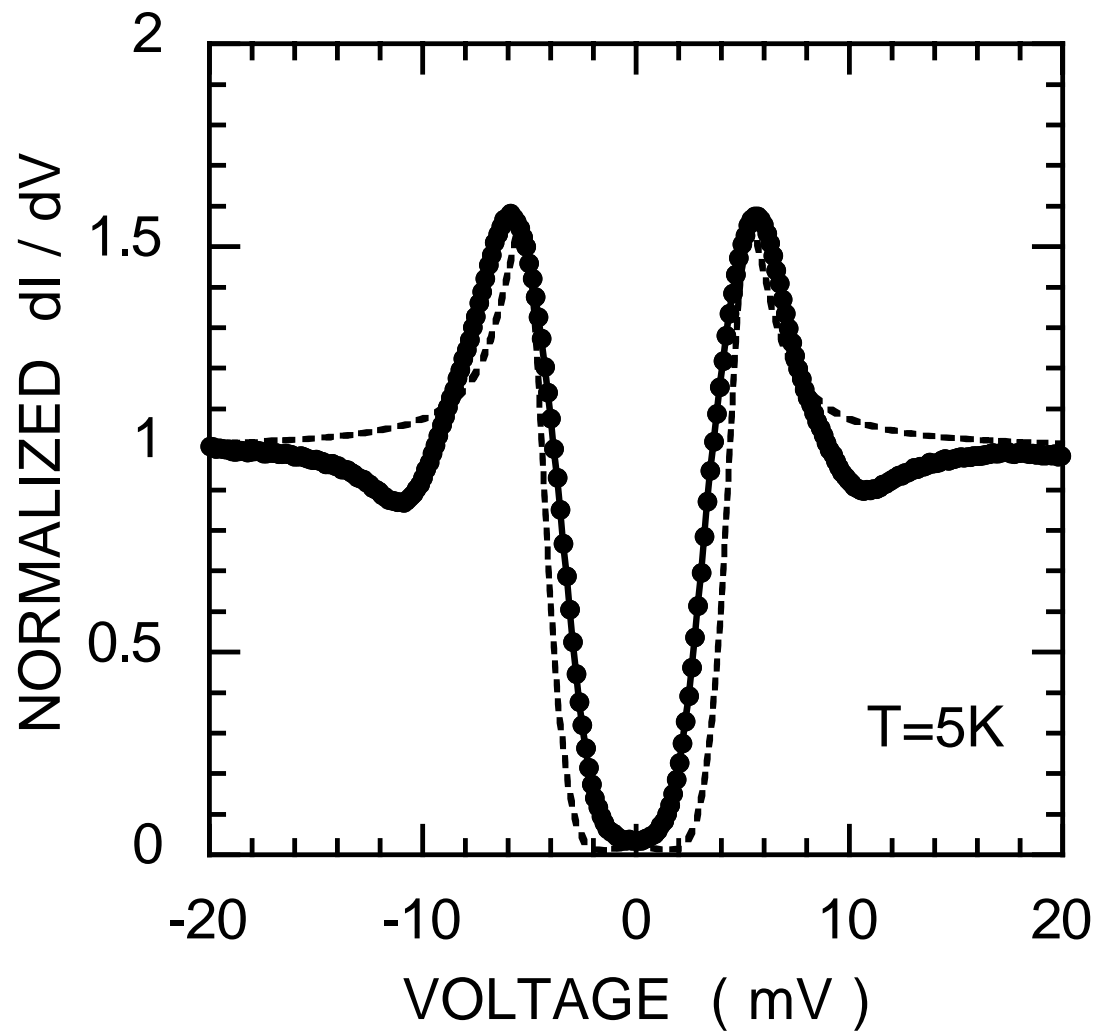


Figure 4
Heitmann et al

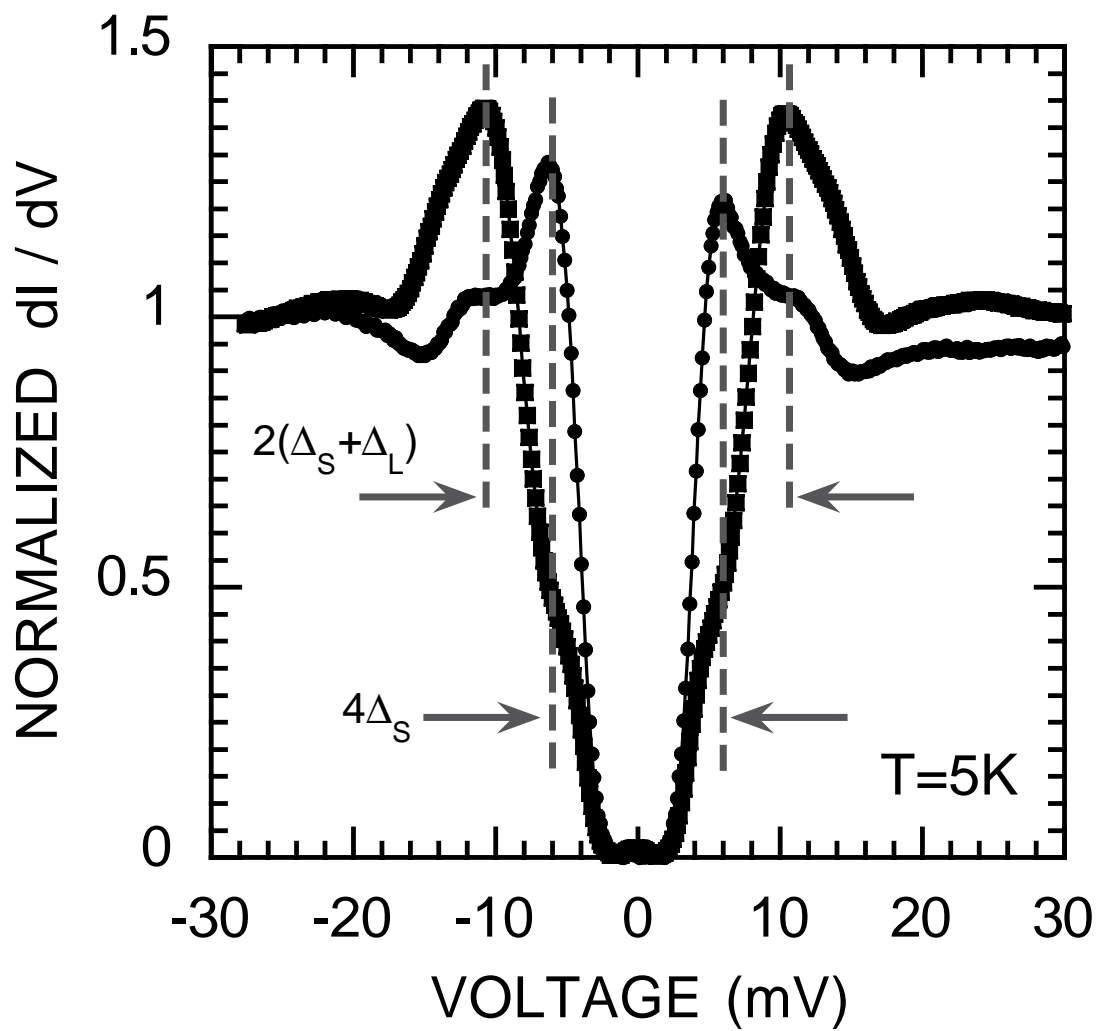


Figure 5
Heitmann et al

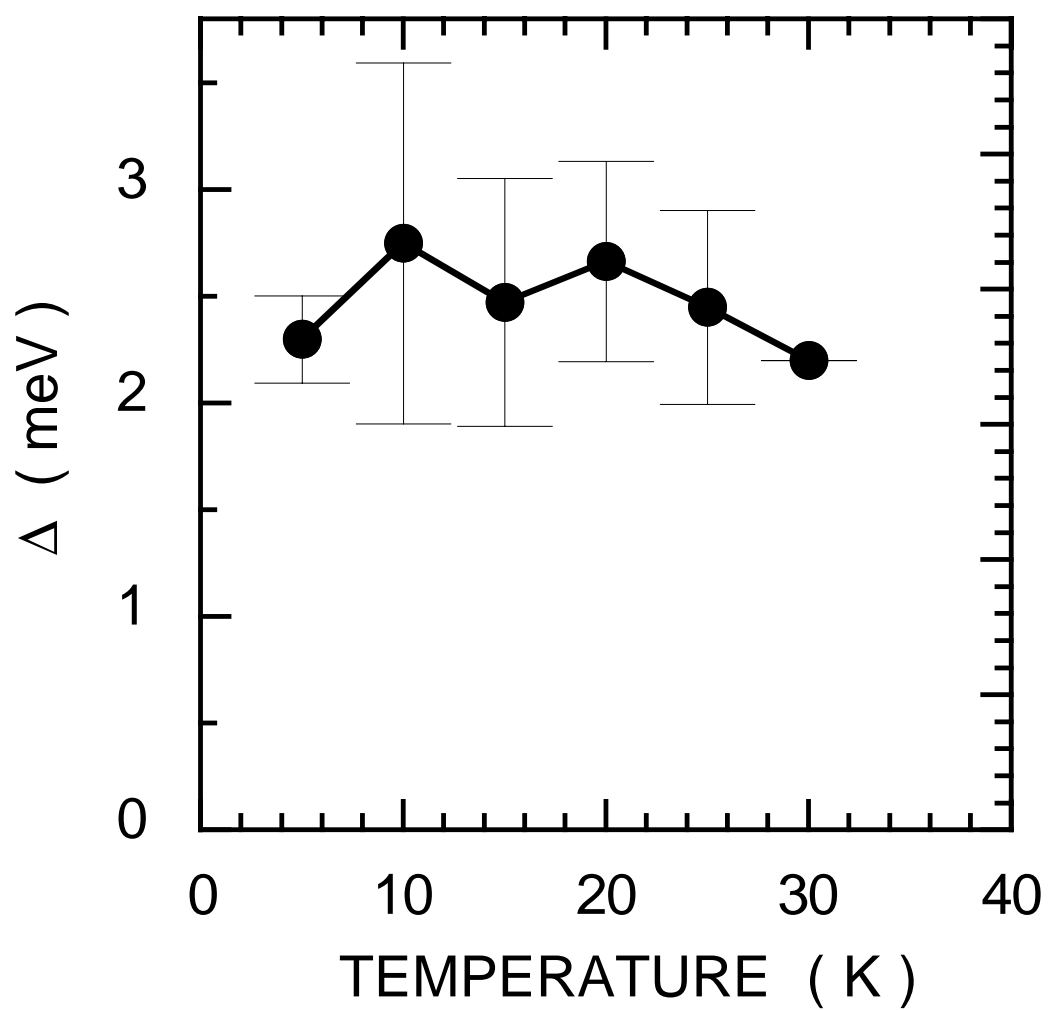


Figure 6
Heitmann et al

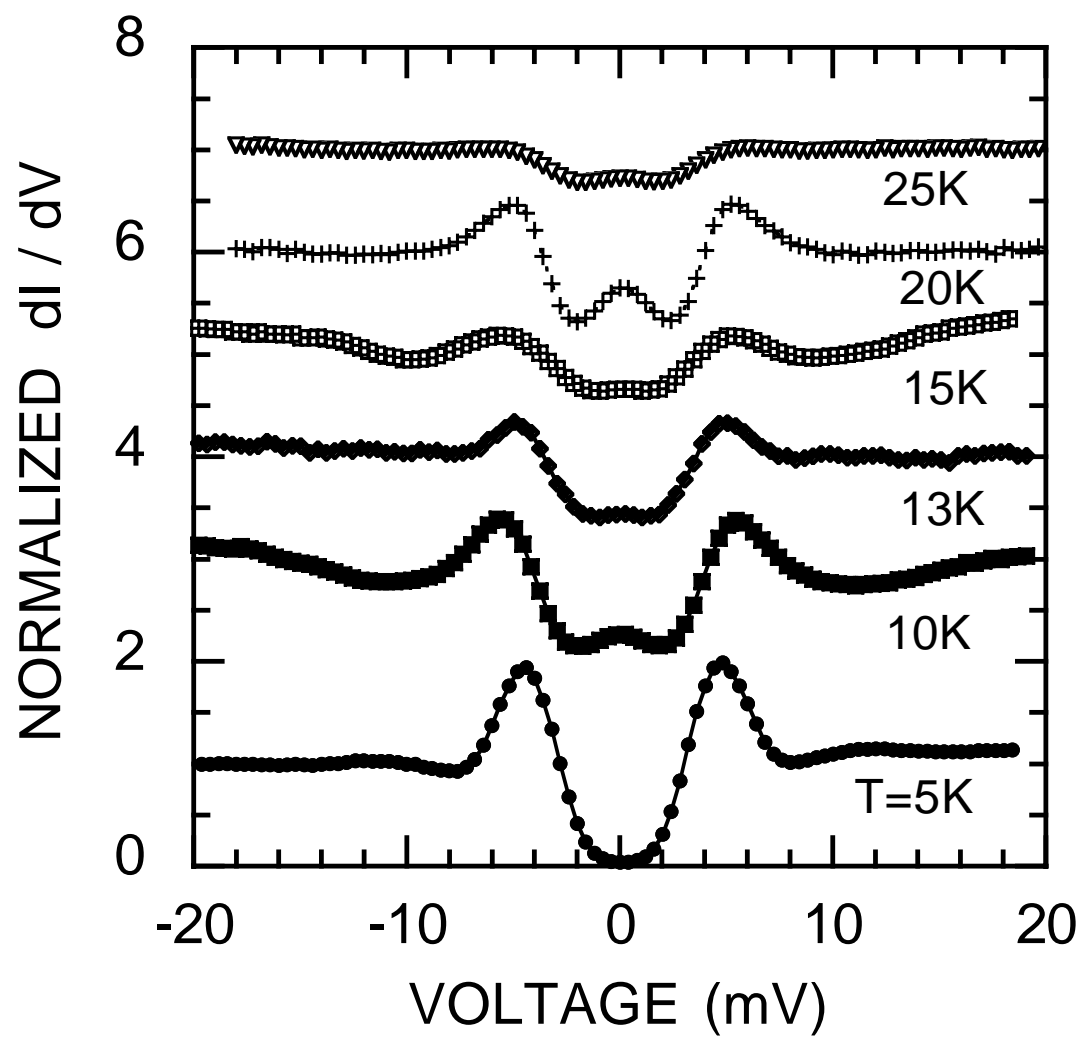


Figure 7
Heitmann et al

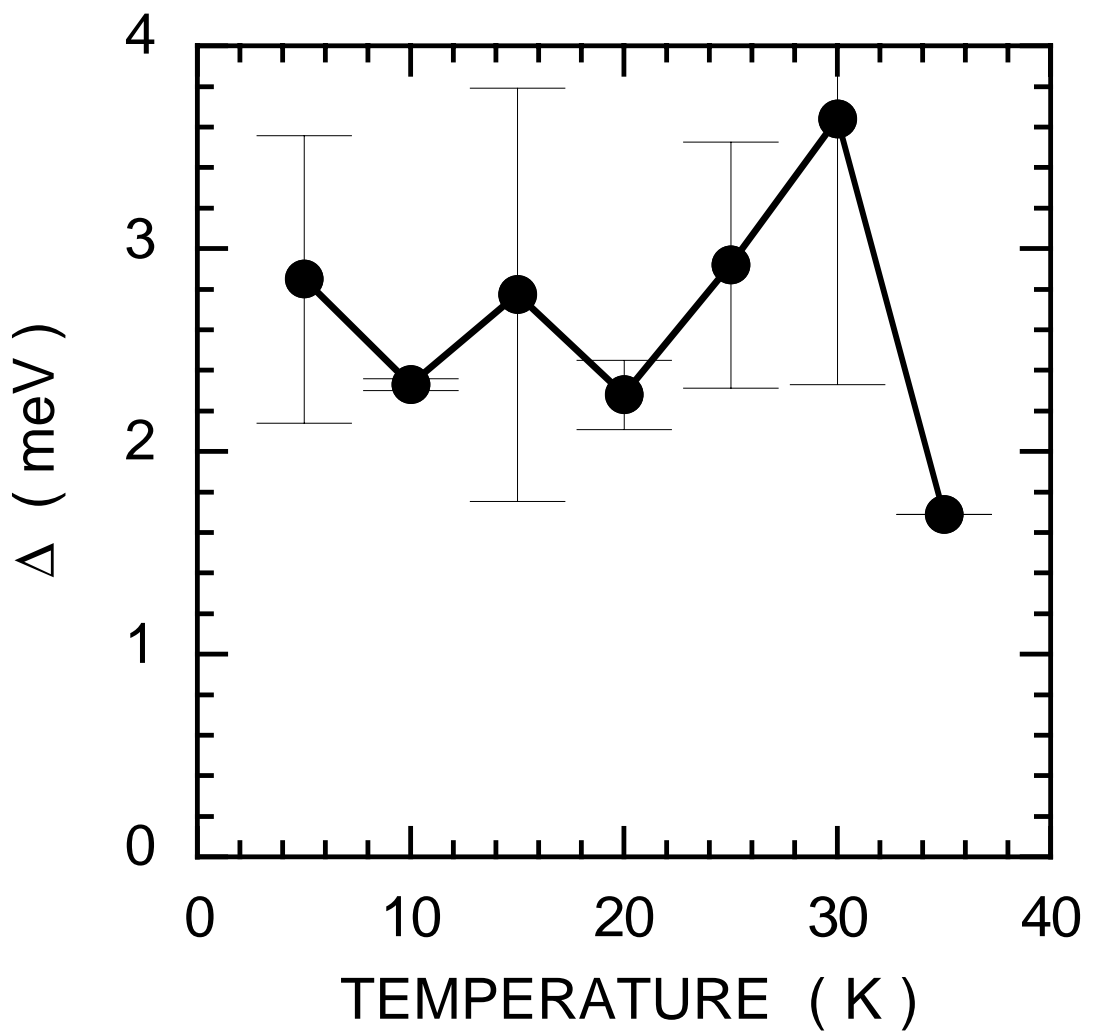


Figure 8
Heitmann et al

